Improved estimations of the plastic zones ahead of crack tips using linear elastic fracture mechanics concepts

Habib Zambrano Rodríguez
Department of Engineering Design and Materials, Norwegian University of Science and Technology, Trondheim – Norway

Jaime Tupiassú Pinho de Castro, Marco Antonio Meggiolaro
Department of Mechanical Engineering, Pontifical Catholic University of Rio de Janeiro, Rio de Janeiro/RJ – Brazil

Abstract

Crack tip plastic zones can be and usually are severely underestimated at the high load levels associated with the yield safety factors $1.2 < \varphi_Y < 3$ typically used in the design of tough metallic structures. This happens because the stress field around the tip is supposed to be solely controlled by the stress intensity factor, neglecting the significant effect of the nominal stress to the yield strength ratio, σ_n/S_Y. Since most Fracture Mechanics design methods use plastic zone size estimates and stress intensity similitude assumptions, this fact is more than an academic issue, it is a matter of great practical interest. This problem is demonstrated by using Inglis or Westergaard stress functions to generate the complete stress field around the crack tip in an infinite plate considering in an appropriate way the important σ_n/S_Y effects.

Keywords: Fracture Mechanics, plastic zone estimates, nominal stress effects.

1 Introduction

For both academic and design purposes, the plastic zones size and shape $pz(\theta)$ ahead of a crack tip are traditionally estimated from simplified linear elastic (LE) stress analysis, assuming that the stress field depends only on the stress intensity factor (SIF) K_I (or K_{II} or K_{III}). For example, assuming that $\sigma_{ij} = [K_I] \cdot [1/\sqrt{(2\pi r)}] \cdot [f_{ij}(\theta)] = f(K_I)$, where r is the distance from the crack tip, θ is the angle measured from the crack plane and $f_{ij}(\theta)$ are the mode I Williams θ-functions, and equating the resulting Mises stress to S_Y, the yielding strength, the simplest elastic-plastic frontiers in plane stress and in plane strain are estimated by [1].

Mechanics of Solids in Brazil 2009, H.S. da Costa Mattos & Marcílio Alves (Editors)
Brazilian Society of Mechanical Sciences and Engineering, ISBN XXX-XX-XXXXX-XX-X

$$pz(\theta)_{pl-\sigma} = (K_I^2/2\pi S_Y^2) \cdot \cos^2(\theta/2) \cdot [1 + 3\sin^2(\theta/2)]$$
$$pz(\theta)_{pl-\varepsilon} = (K_I^2/2\pi S_Y^2) \cdot \cos^2(\theta/2) \cdot [(1-2\nu)^2 + 3\sin^2(\theta/2)] \quad (1)$$

where ν is Poisson's coefficient. Thus, according to this simplified estimate, the plastic zone size directly ahead of a crack tip in plane stress should be $pz(0)_{pl-\sigma} = pz_0 = (1/2\pi)(K_I/S_Y)^2$. This value is the reference used to normalize all the plastic zone plots presented below.

However, the classical $\sigma_{ij} = f(K_I)$ hypothesis almost universally used in LEFM analysis is only valid very close to the crack tip, more specifically if $r \to 0$, exactly where the assumed elastic behavior breaks down. In particular, this approximation predicts that the normal stress perpendicular to the crack plane in a Griffith plate is $\sigma_y(x \to \infty, y = 0) = 0$, instead of $\sigma_y(x \to \infty, y = 0) = \sigma_n$, as it should. Therefore, the classical $\sigma_{ij} = f(K_I)$ hypothesis does ***not*** obey all the plate boundary conditions (this same problem, by the way, also happens with the more elaborated HRR elastic-plastic field.) Therefore, as the plastic zone borders are not necessarily (neither are usually) too close to the crack tip, it is worth to at least estimate the effect of the nominal stress to the yield strength ratio σ_n/S_Y on $pz(\theta)$, instead of simply neglecting it.

A quite simple, but certainly not unreasonable first estimate of the σ_n/S_Y effect on the plastic zones frontiers around the crack tips can be made by forcing $\sigma_y(x \to \infty, y = 0) = \sigma_n$, adding up a constant $\sigma_y = \sigma_n$ stress to the Williams (or Irwin) stress LE field to obtain

$$\sigma(\theta)^{Williams+\sigma_n}_{Mises,pl-\sigma} = \sigma(\theta)^{Wil+\sigma_n}_{M,pl-\sigma} = [(\kappa f_x)^2 + (\kappa f_y + \sigma_n)^2 - (\kappa f_x)(\kappa f_y + \sigma_n) + 3(\kappa f_{xy})^2]^{1/2} \quad (2)$$

where $\sigma(\theta)^{Wil+\sigma_n}_{M,pl-\sigma}$ is the resulting LE Mises stress distribution around the crack tip in plane stress (considering the σ_n/S_Y effect), $\kappa = K_I/\sqrt{(2\pi r)}$, and f_x, f_y and f_{xy} are the θ-functions associated with the σ_x, σ_y and τ_{xy} Williams (or Irwin) stresses in mode I. Equating $\sigma(\theta)^{Wil+\sigma_n}_{M,pl-\sigma} = S_Y$ and repeating the process for plane strain, $pz(\theta)^{Wil+\sigma_n}_{M,pl-\sigma} \Big/ pz_0$ and $pz(\theta)^{Wil+\sigma_n}_{M,pl-\varepsilon} \Big/ pz_0$ plots can be generated to enhance the searched σ_n/S_Y effect, as shown in Figure 1.

Figure 1 indicates that the estimated σ_n/S_Y influence on the size and the shape of the plastic zones that surround the crack tips under real normal loading conditions, which can reach ratios $\sigma_n/S_Y > 0.8$ in structures designed for minimum weight, is clearly not negligible. However, it cannot be prove that the σ_n/S_Y effects are really that important, since the hypothesis used to generate its plots is not mathematically sound. But this simple estimate nevertheless points out that the plastic zone dependence on σ_n/S_Y should be studied in a more careful way, as done in the following sections.

2 Plastic zones estimated using the Inglis stresses

A much better estimate for the σ_n/S_Y influence on the size and shape of the plastic zones $pz(\theta)$ can be generated by using the classical Inglis stress field in an infinite plate with a crack-like very sharp elliptical notch, with its major semi-axis a perpendicular to the tensile nominal stress σ_n, and with its minor semi-axis $b << a$.

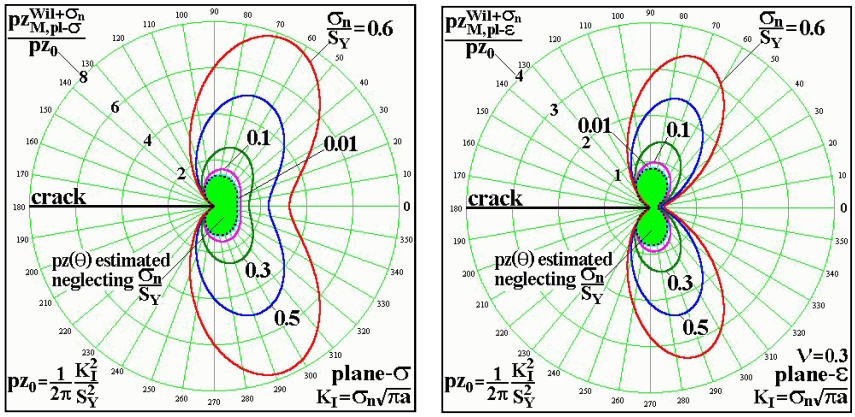

Figure 1: Mode I plastic zones estimated for the infinite cracked plate, which has $K_I = \sigma_n\sqrt{(\pi a)}$, by summing σ_n to the Williams $\sigma_y(K_I)$ stress, to force σ_y (σ_n far from the crack tips.

Therefore, making $x = c{\cdot}\cosh\alpha{\cdot}\cos\beta$ and $y = c{\cdot}\sinh\alpha{\cdot}\sin\beta$, such a crack-like sharp notch is quite simply described in elliptical coordinates (α,β) by $\alpha = \alpha_0$, where $a = c{\cdot}\cosh\alpha_0$, $b = c{\cdot}\sinh\alpha_0$, and $c = a/\cos\alpha_0$. The linear elastic stresses in the Inglis plate loaded by a general bi-axial nominal stress field are given by the following infinite series [2, 3]

$$\begin{aligned}\sigma_\alpha = \gamma\sum_n A_n\{&(n+1)e^{(1-n)\alpha}\cos(n+3)\beta + (n-1)e^{-(n+1)\alpha}\cos(n-3)\beta -\\ &-[4e^{-(n+1)\alpha} + (n+3)e^{(3-n)\alpha}]\cos(n+1)\beta + [4e^{(1-n)\alpha} + (3-n)e^{-(n+3)\alpha}]\cos(n-1)\beta\} +\\ &+B_n\{e^{-(n+1)\alpha}[n\cos(n+3)\beta + (n+2)\cos(n-1)\beta] - [(n+2)e^{(1-n)\alpha} + ne^{-(n+3)\alpha}]\cos(n+1)\beta\}\end{aligned} \tag{3}$$

$$\begin{aligned}\sigma_\beta = \gamma\sum_n A_n\{&(3-n)e^{(1-n)\alpha}\cos(n+3)\beta - (n+3)e^{-(n+1)\alpha}\cos(n-3)\beta -\\ &-[4e^{-(n+1)\alpha} - (n-1)e^{(3-n)\alpha}]\cos(n+1)\beta + [4e^{(1-n)\alpha} + (n+1)e^{-(n+3)\alpha}]\cos(n-1)\beta\} -\\ &-B_n\{e^{-(n+1)\alpha}[n\cos(n+3)\beta + (n+2)\cos(n-1)\beta] - [(n+2)e^{(1-n)\alpha} + ne^{-(n+3)\alpha}]\cos(n+1)\beta\}\end{aligned} \tag{4}$$

$$\begin{aligned}\tau_{\alpha\beta} = \gamma\sum_n A_n\{&(n-1)e^{(1-n)\alpha}\sin(n+3)\beta + (n+1)e^{-(n+1)\alpha}\sin(n-3)\beta - (n+1)e^{(3-n)\alpha}]\sin(n+1)\beta -\\ &-(n-1)e^{-(n+3)\alpha}]\sin(n-1)\beta\} -\\ &-B_n\{e^{-(n+1)\alpha}[n\sin(n+3)\beta + (n+2)\sin(n-1)\beta] - [(n+2)e^{(1-n)\alpha} + ne^{-(n+3)\alpha}]\sin(n+1)\beta\}\end{aligned} \tag{5}$$

where $\gamma = (\cosh 2\alpha - \cos 2\beta)^{-2}$ and n is an integer.

Fortunately, only 5 of these infinite series constants are non-zero when the Inglis plate is loaded by a simpler uni-axial tensile stress σ_n perpendicular to the elliptical hole major axis, namely

$$\begin{cases} \mathbf{A_1} = -\sigma_\mathbf{n}[\mathbf{1} + \mathbf{2exp}(\mathbf{2}\alpha_\mathbf{0})] \\ \mathbf{A_{-1}} = \sigma_\mathbf{n}/16 \\ \mathbf{B_1} = \sigma_\mathbf{n}\mathbf{exp}(\mathbf{4}\alpha_\mathbf{0}) \\ \mathbf{B_{-1}} = \sigma_\mathbf{n}(\mathbf{1} + \mathbf{cosh2}\alpha_\mathbf{0}) \\ B_{-3} = \sigma_n/8 \end{cases} \tag{6}$$

Modeling the crack as a very sharp elliptical notch, with a tiny but nevertheless finite tip radius estimated as half the crack tip opening displacement, $\rho = b^2/a = CTOD/2 = 2K_I{}^2/\pi S_Y E'$, where $E' = E$ in plane stress and $E' = E/(1 - \nu^2)$ in plane strain, and knowing that whereas the cracked infinite plate has a SIF $K_I = \sigma_n\sqrt{(\pi a)}$, the notched one has a corresponding stress concentration factor $K_t = 1 + 2a/b$, then

$$K_t = 1 + 2 \cdot \frac{a}{b} = 1 + 2\sqrt{\frac{a}{\rho}} = 1 + 2 \cdot \sqrt{\frac{a\pi E' S_Y}{2 \cdot \sigma_n^2 \pi a}} \Rightarrow \frac{a}{b} = \sqrt{\frac{E'}{2 \cdot \sigma_n} \cdot \frac{S_Y}{\sigma_n}} = \sqrt{\frac{E'\phi_Y}{2 \cdot \sigma_n}} \tag{7}$$

where $\varphi_Y = S_Y/\sigma_n$ is its nominal safety factor against yielding. Using this a/b ratio to obtain the notch shape that simulates the crack by $\alpha_0 = tanh^{-1}(b/a)$, then the LE stresses in the cracked plate can be calculated substituting the 5 constants specified above in (3-5), a tedious but certainly not a difficult task. Finally, the Mises stress resulting from σ_α, σ_β, $\tau_{\alpha\beta}$, and (in the plane strain case) $\sigma_z = \nu(\sigma_\alpha + \sigma_\beta)$ can be used to estimate the Inglis plastic zones by numerically solving equations (8-9) for $|\theta| \leq \pi$:

$$\sigma^{Ing}_{M,pl-\sigma} = \sqrt{\sigma_\alpha^2 + \sigma_\beta^2 - \sigma_\alpha\sigma_\beta + 3\tau_{\alpha\beta}^2} = S_Y \tag{8}$$

$$\sigma^{Ing}_{M,pl-\varepsilon} = \sqrt{0.5[(\sigma_\alpha - \sigma_\beta)^2 + (\sigma_\alpha - \sigma_z)^2 + (\sigma_z - \sigma_\beta)^2] + 3\tau_{\alpha\beta}^2} = S_Y \tag{9}$$

Some resulting $pz(\theta)^{Ing}_{M,pl-\sigma}\Big/pz_0$ and $pz(\theta)^{Ing}_{M,pl-\varepsilon}\Big/pz_0$ frontiers, obtained from the numerical solution of equations (8) and (9), are shown in Figure 2.

Therefore, the influence of the nominal stress to the yield strength ratio on the plastic zones, although a little less than estimated by the simple approximation presented in Figure 1, is indeed significant and should not be neglected in practical applications. This is a strong assertion, but it is supported by the exact LE stress field solution for the infinite cracked plate in mode I, when the crack is modeled as an elliptical sharp notch of tip radius $\rho = CTOD/2$, a quite reasonable hypothesis. Nevertheless, it is worth to use an alternative approach to confirm it, as follows.

3 Plastic zones estimated using the Westergaard stress function

The appropriate use of an adequate Westergaard $Z(z)$ stress function provides an alternative way to rigorously estimate the size and the shape of the plastic zones ahead of crack tips departing from the LE stress field. However, since the elastic-plastic frontier is not adjacent to the crack tip, the full

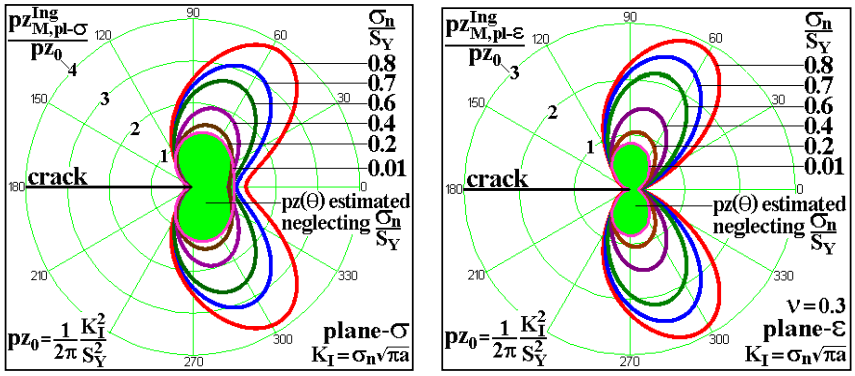

Figure 2: Mises plastic zones in plane stress and in plane strain, calculated using the Inglis linear elastic stress field in an infinite cracked plate loaded in mode I, modeling the crack as a very sharp elliptical notch of tip radius ρ = *CTOD/2* (avoiding in this way the physically unrealistic singularity at the crack tip).

stresses generated from $Z(z)$ must be used in such a calculation. This can be easily demonstrated by revisiting the classical Irwin solution for the cracked infinite plate loaded in mode I.

Thus, if (x, y) and *(r, θ)* are the Cartesian and the polar coordinates centered at the crack tip, *i* = $\sqrt{-1}$ is the complex unity and *z = x + iy* is a complex variable, the Irwin solution is obtained from the Westergaard stress function [4–6]

$$Z(z) = z\sigma_n/\sqrt{(z^2 - a^2)} \Rightarrow Z'(z) = dZ/dz = -a^2\sigma_n/(z^2 - a^2)^{3/2} \tag{10}$$

The linear elastic stresses around the crack tip can be calculated from the stress function $Z(z)$ and from its derivative *Z'(z)* by

$$\begin{cases} \sigma_x = \mathrm{Re}(Z) - y\,\mathrm{Im}(Z') - \sigma_n \\ \sigma_y = \mathrm{Re}(Z) + y\,\mathrm{Im}(Z') \\ \tau_{xy} = -y\,\mathrm{Re}(Z') \end{cases} \tag{11}$$

Note that to solve the mode I problem from $Z(z)$, a constant term *-σ_n* has to be summed to the *σ_x = Re(Z) - yIm(Z')* formula to force *$\sigma_x(\infty)$ = 0* in the plate, an adequate mathematical trick since a constant stress in the x direction does not affect the stress field near the crack tip. However, the *σ_y = Re(Z) - y·Im(Z')* stress is usually approximated to generate a stress intensity factor (generally a highly desirable feature but not for estimating *pz(θ)*, since it neglects the *σ_n/S_Y* influence far from the crack tip) by writing

$$\sigma_y(\theta = 0) = \sigma_n(x + a)/[(x + a)^2 - a^2]^{1/2} \cong \sigma_n a/\sqrt{(2ax)} = K_I/\sqrt{(2\pi r)} \quad (\text{if } x << a) \tag{12}$$

where *2a* is the crack size perpendicular to the nominal tensile stress σ_n.

Note that equation (12) yields $\sigma_y(\theta = 0) = K_I/\sqrt{(2\pi r)} = 0$ if $r \to \infty$, thus it does ***not*** generate the stress far from the crack tip. Thus this classical approximation cannot be used to study the σ_n/S_Y influence on $pz(\theta)$, which is not too close to the crack tip. But this task can be fulfilled by first rewriting Z and Z' in polar coordinates centered at the crack tip

$$Z = \frac{[a + (r \cdot \cos\theta) + i\,(r \cdot \sin\theta)] \cdot \sigma_n}{\sqrt{[a + (r \cdot \cos\theta) + i\,(r \cdot \sin\theta)]^2 - a^2}} \Rightarrow Z' = \frac{-a^2 \cdot \sigma_n}{\left\{[a + (r \cdot \cos\theta) + i\,(r \cdot \sin\theta)]^2 - a^2\right\}^{3/2}} \tag{13}$$

and then by using the ***complete*** stress field generated from Z and Z' to calculate the resulting Mises (or Tresca, for that matter) stress. This equivalent stress is then equated to the yielding strength to obtain the required $pz(\theta)$ elastic-plastic frontiers considering the σ_n/S_Y effect. For example, in plane stress this procedure generates equation (14). The same process can be easily applied for plane strain case. The numerical solution of equation (14) generates the required Westergaard elastic-plastic frontier $pz(\theta)^{Wtg}_{M,pl-\sigma}\Big/pz_0$, see Figure 3. And the corresponding equation for the plane strain case can also be numerically solved to generate $pz(\theta)^{Wtg}_{M,pl-\sigma}\Big/pz_0$, as also shown in Figure 3.

Note that these estimates for the elastic-plastic frontiers based on the Westergaard stress function, like the estimates based on the Inglis stresses obtained above, are mathematically sound, indicating that the claimed σ_n/S_Y effect on $pz(\theta)$ is indeed significant, and should not be neglected.

$$\begin{aligned}
&\left\{\left[\mathrm{Re}\left(\frac{(a+r\cdot\cos\theta+i\cdot r\sin\theta)\cdot\sigma_n}{\sqrt{(a+r\cdot\cos\theta+i\cdot r\sin\theta)^2-a^2}}\right) - y\,\mathrm{Im}\left(\frac{-a^2\cdot\sigma_n}{\left[(a+r\cdot\cos\theta+i\cdot r\sin\theta)^2-a^2\right]^{3/2}}\right) - \sigma_n\right]^2 + \right.\\
&\quad + \left[\mathrm{Re}\left(\frac{(a+r\cdot\cos\theta+i\cdot r\sin\theta)\cdot\sigma_n}{\sqrt{(a+r\cdot\cos\theta+i\cdot r\sin\theta)^2-a^2}}\right) + y\,\mathrm{Im}\left(\frac{-a^2\cdot\sigma_n}{\left[(a+r\cdot\cos\theta+i\cdot r\sin\theta)^2-a^2\right]^{3/2}}\right)\right]^2 -\\
&\quad - \left[\mathrm{Re}\left(\frac{(a+r\cdot\cos\theta+i\cdot r\sin\theta)\cdot\sigma_n}{\sqrt{(a+r\cdot\cos\theta+i\cdot r\sin\theta)^2-a^2}}\right) - y\,\mathrm{Im}\left(\frac{-a^2\cdot\sigma_n}{\left[(a+r\cdot\cos\theta+i\cdot r\sin\theta)^2-a^2\right]^{3/2}}\right) - \sigma_n\right]\cdot\\
&\quad \cdot \left[\mathrm{Re}\left(\frac{(a+r\cdot\cos\theta+i\cdot r\sin\theta)\cdot\sigma_n}{\sqrt{(a+r\cdot\cos\theta+i\cdot r\sin\theta)^2-a^2}}\right) + y\,\mathrm{Im}\left(\frac{-a^2\cdot\sigma_n}{\left[(a+r\cdot\cos\theta+i\cdot r\sin\theta)^2-a^2\right]^{3/2}}\right)\right] +\\
&\quad \left. +3\cdot\left[-y\,\mathrm{Re}\left(\frac{-a^2\cdot\sigma_n}{\left[(a+r\cdot\cos\theta+i\cdot r\sin\theta)^2-a^2\right]^{3/2}}\right)\right]^2\right\}^{1/2} = S_Y
\end{aligned} \tag{14}$$

4 Comparing the plastic zones estimated from Inglis and from Westergaard

Figure 4 compares the Mises plastic zones calculated using the Inglis stresses assuming that the crack is a very sharp elliptical notch of tip radius $\rho = CTOD/2$, and the complete stresses generated by the Westergaard stress function, without the simplification required to obtain the classical $K_I = \sigma\sqrt{(\pi a)}$ formula.

As $pz_{Ing}(\theta)$ and $pz_{Wtg}(\theta)$ are obtained from completely different equations, their near coincidence is certainly not fortuitous. Therefore, the large σ_n/S_Y effect predicted by these rigorous solutions really

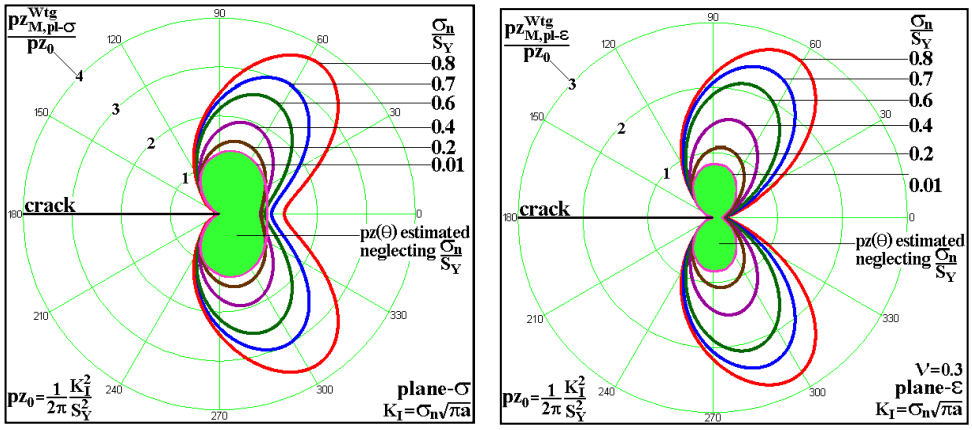

Figure 3: Mises plastic zones in plane stress and in plane strain in an infinite cracked plate in mode I, calculated using the complete stresses generated by the Westergaard stress function.

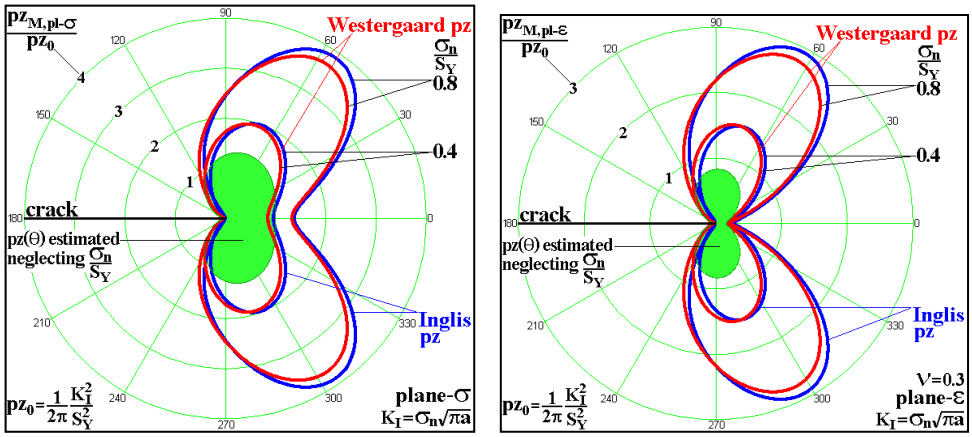

Figure 4: Comparison of the Mises plastic zones estimated from Inglis (using ρ = *CTOD/2*) and from Westergaard under plane stress and plane strain.

should not be neglected in practice. This point must be emphasized, since it is the plastic zone size that ***validates*** most LEFM predictions. Moreover, the Inglis and Westergaard plastic zones virtually coincide when the sharp ellipsis used to model the crack has its minor semi-axis (instead of its tip radius) assumed as half the classical crack opening displacement estimated by Irwin, $b = CTOD/2 = 2K_I^2/\pi S_Y E'$, see Figure 5.

It is interesting to note that assuming the Inglis and the Westergaard-based $pz(\theta)$ must coincide, a

quite reasonable hypothesis since they describe the same linear elastic problem, then a new estimate for the *CTOD* can be proposed, since if $b = 2K_I^2/\pi S_Y E'$ and $\rho = b^2/a$, then

$$CTOD = 2\rho = 2\frac{4K_I^4}{(\pi S_Y E')^2 \cdot a} = \frac{8}{\pi}\left(\frac{K_I \sigma_n}{E' S_Y}\right)^2 = \frac{8}{\pi}\left(\frac{K_I}{E'}\phi_Y\right)^2 \cong 2.55\left(\frac{K_I}{E'}\phi_Y\right)^2 \tag{15}$$

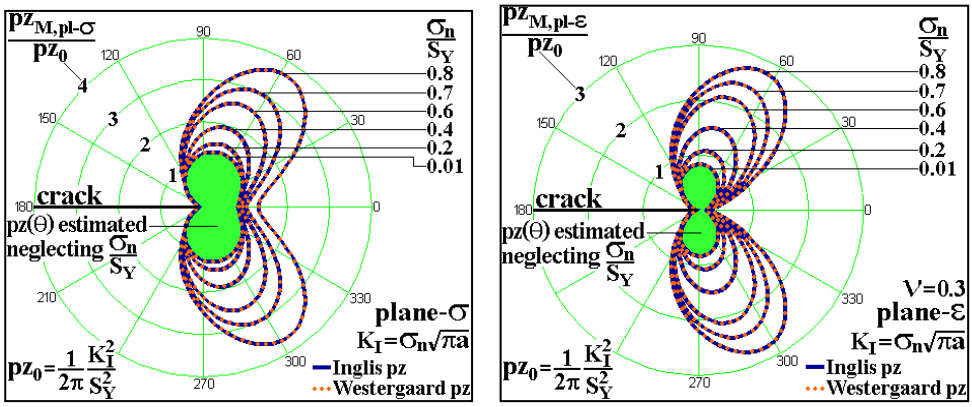

Figure 5: The plastic zones estimated using the complete linear elastic stresses induced by the Westergaard stress function are visually undistinguishable from the plastic zones estimated from the Inglis stresses when a sharp elliptical notch with $b = CTOD/2 = 2K_I^2/\pi S_Y E'$ instead of $\rho = CTOD/2$ is used to model the crack.

5 Corrected plastic zone estimates including equilibrium considerations

The so-called Inglis and Westergaard plastic zones are already an improvement over the traditional $pz(\theta)$ estimates based solely on K_I, such as those expressed in equations (1). They take into account the σ_n/S_Y effect which, as demonstrated above, is indeed quite important under real loading conditions, where yielding safety factors in the range $1.2 < S_Y/\sigma_n = \varphi_Y < 3$ are common practice when designing and using tough metallic structures. But they can be further enhanced because, in spite of obeying all contour conditions, they intrinsically suppose that the stresses remain LE in the whole studied plate, neglecting the yielding near the crack tip. In other words, they do not consider the force loss caused by the yielding-induced stress limitation inside the plastic zone and, in consequence, they violate the equilibrium equation.

This problem can, of course, be corrected following Irwin's classical idea, assuming that:

1. the material does not strain harden, thus the Mises (or Tresca) stress remains fixed inside the plastic zone, where $\sigma_M = S_Y$; and

2. the original LE stress distribution can be simply displaced by a value $r^*(\theta)$ to balance the force originally associated with $\sigma_M(r, \theta) > S_Y$ or, in other words, the LE stresses outside the plastic zone can be expressed by $\sigma_{ij}(r - r^*(\theta), \theta)$.

The Irwin plastic zone $pz_{Irw}(\theta)$, which is corrected following his two assumptions to balance the force generated bythe K_I-induced σ_y stress, is generally calculated only at the crack plane, where $pz_{Irw}(\theta = 0) = K_I{}^2/\pi S_Y{}^2 = 2pz_0$. But his idea can be easily extended to generate the whole $pz_{Irw}(\theta)$ elastic-plastic frontier by solving $\sigma_M(r = pz_{Irw}(\theta), \theta) = S_Y$, a task that can be accomplished by first calculating the σ_y linear elastic stress at the classical $pz(\theta)$ frontier described by equation (1):

$$\sigma_y[pz(\theta), \theta] = \frac{K_I}{\sqrt{2\pi \cdot pz(\theta)}} \cos\frac{\theta}{2}\left[1 + sin\frac{\theta}{2} sin\frac{3\theta}{2}\right] \tag{16}$$

This $\sigma_y(\theta)$ stress at the $pz(\theta)$ frontier must remain constant inside $pz_{Irw}(\theta)$, since Irwin assumed that the material does not strain-harden, but it must also generate the same force caused by the singular LE $\sigma_y(\theta)$ original stress to maintain the plate under equilibrium (neglecting the σ_n/S_Y ratio contribution), thus

$$\sigma_y(r = pz(\theta), \theta) \cdot zp_{Irw}(r, \theta) = \int_0^{pz(\theta)} \left[\frac{K_I}{\sqrt{2\pi r}} \cos\frac{\theta}{2}\left(1 + \sin\frac{\theta}{2}\sin\frac{3\theta}{2}\right)\right] dr \tag{17}$$

Therefore, the classical $pz_{Irw}(\theta)$ in plane stress can be expressed by an unique analytical expression:

$$pz_{Irw}(\theta) = \frac{2K_I\sqrt{pz(\theta)}}{\sqrt{2\pi} \cdot \sigma_y[pz(\theta), \theta]} \cos\frac{\theta}{2}\left[1 + sin\frac{\theta}{2} sin\frac{3\theta}{2}\right] \tag{18}$$

It is relatively simple to reproduce this analysis to treat the plane strain case, see Figure 6. As expected, the $pz_{Irw}(\theta)$ are just σ_n/S_Y-independent hypertrophied versions of the traditionally estimated K_I-induced $pz(\theta)$ plastic zones.

Now Irwin's idea can be finally adapted to estimate the Mises plastic zones around a crack tip using the complete stresses generated by the Westergaard stress function, obeying at the same time the contour condition $\sigma_y(x \rightarrow \infty) = \sigma_n$ and the equilibrium of the applied force on the Irwin plate, as any decent estimate should always do. It is interesting to note that it is not necessary to repeat this exercise departing from the Inglis stresses, since the plastic zones generated from them are almost identical to the Westergaard plastic zones, $pz_{Ing}(\theta) \cong pz_{Wtg}(\theta)$ if $b = 2K_I{}^2/\pi S_Y E'$, as demonstrated above.

A procedure very similar to the one used for generating equation (18), based on the assumption that the $\sigma_y(\theta)$ stress remain fixed inside the plastic zone because the material does not strain-harden, can be applied to accomplish this purpose:

$$\begin{gathered} \sigma_y[pz_{Wtg}(\theta), \theta] \cdot pz_{eql}(\theta) = \int_0^{pz_{Wtg}(\theta)} \sigma_y(r, \theta) dr \Rightarrow \\ pz_{eql}(\theta) = \frac{1}{\sigma_y[zp_{Wtg}(\theta), \theta]} \int_0^{pz_{Wtg}(\theta)} \left\{\mathrm{Re}[Z(r, \theta)] + y\,\mathrm{Im}'[Z'(r, \theta)]\right\} dr \end{gathered} \tag{19}$$

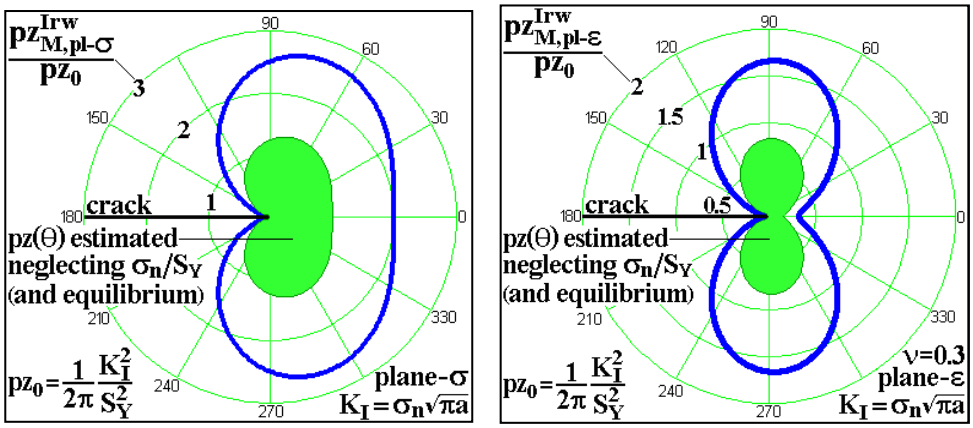

Figure 6: Irwin plastic zones $pz_{Irw}(\theta)$ in plane stress and plane strain, generated to balance the force generated by the K_I-induced σ_y stress, without taking into account the σ_n/S_Y effects.

The resulting plastic zone estimates, $pz_{eql}(\theta)$, for the cracked infinite plate loaded in mode I in plane stress and in plane strain considering both the σ_n/S_Y ratio ***and*** the equilibrium influence, can then be finally obtained by numerically integrating equation (19), see Figure 7.

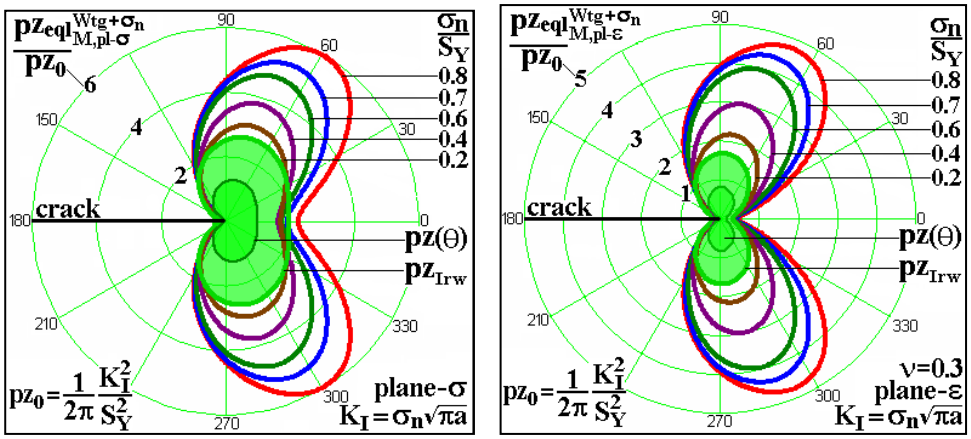

Figure 7: Mises $pz(\theta)$ estimated using the complete stresses induced by the Westergaard stress function for the Griffith plate, considering both the σ_n/S_Y ratio ***and*** the equilibrium effects.

Figure 7 presents the best plastic zones that can be estimated from the linear elastic stress field in a cracked Irwin plate, neglecting strain-hardening but considering both the nominal stress to the yield

strength ratio σ_n/S_Y and the force equilibrium effects, based on relatively simple but sound analytical procedures. It is important to note that at $\sigma_n/S_Y = 0.8$ the maximum dimension of this $pz_{eql}(\theta)$ in plane stress is about 6 (six) times bigger than the frequently used classical $pz_0 = K_I^2/2\pi S_Y^2$ estimate, whereas in plane strain it is almost 5 times bigger, values that certainly are not negligible.

And it is worth mentioning that these simple estimates do reproduce the familiar butterfly shape of the plastic zone around the crack tip, well known by anyone who ever made a fatigue crack propagation or a toughness measurement using a polished specimen.

6 Fitting the equilibrated plastic zone estimates

It is interesting to propose empirical equations to fit the obtained numerical solutions of the analytically proposed plastic zone frontiers which consider both the σ_n/S_Y and the equilibrium effects. The plastic zone size at an angle $\theta = 0$ can be expressed for $0 \leq \sigma_n/S_Y \leq 0.8$ within 1% by (see Figure 8)

$$\begin{aligned} pz_{eql}(\theta=0)_{pl-\sigma} &= 2pz_0\left[1-0.63\frac{\sigma_n}{S_Y}-0.1\left(\frac{\sigma_n}{S_Y}\right)^2+1.35\left(\frac{\sigma_n}{S_Y}\right)^3\right] \\ pz_{eql}(\theta=0)_{pl-\varepsilon} &= 2pz_0(1-2\nu)^2\left[1-0.17\frac{\sigma_n}{S_Y}-0.3\left(\frac{\sigma_n}{S_Y}\right)^2+1.4\left(\frac{\sigma_n}{S_Y}\right)^3\right] \end{aligned} \tag{20}$$

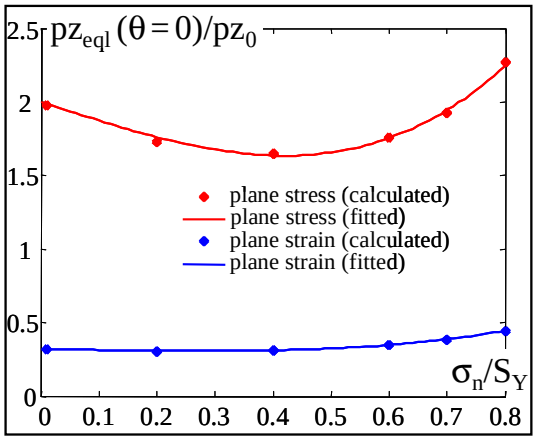

Figure 8: Calculated and fitted values of the equilibrated plastic zone size at the crack plane divided by the reference plastic zone size, $pz_{eql}(\theta = 0)/pz_0$, as a function of the ratio σ_n/S_Y, for the Griffith infinite cracked plate loaded in mode I, for plane stress and plane strain ($\nu = 0.3$).

The above results agree with Finite Element calculations from Newman et al. [7] for elastic-perfectly plastic middle-crack tension specimens M(T), which had thicknesses in the range $1.25 < t < 20mm$, Poisson's ratio $\nu = 0.3$, and a flow stress $\sigma_0 = (S_Y + S_U)/2 = 500MPa$, where S_Y and S_U are the yield and the (tensile) ultimate strength, resulting in the empirical equations

$$pz_{Newman}(\theta = 0) = pz_0 \cdot \frac{\pi^2}{4 \cdot \alpha_g^2} \tag{21}$$

In the plane stress case, associated with a thickness t tending towards zero, the constraint factor α_g clearly tends to 1.15, resulting in $pz_{Newman,pl-\sigma} \cong 1.87 \cdot pz_0$. And under plane strain, assuming a very large t, the above expression tends to $\alpha_g = 2.40$ for the M(T) specimen, therefore $pz_{Newman,pl-\epsilon} \cong 0.43 \cdot pz_0$. For a σ_n/S_Y ratio of 0.7 used in the calculations, equations (20) would result in $pz_{eql,pl-\sigma} = 1.95 \cdot pz_0$ and $pz_{eql,pl-\epsilon} = 0.39 \cdot pz_0$, a quite reasonable agreement.

The maximum size of the plastic zone, pz_{max}, and its associated direction $\theta = \theta_{max}$ can also be fitted with similar expressions for $0 \leq \sigma_n/S_Y \leq 0.8$, resulting in (see Figure 9)

$$\begin{aligned} pz_{eql}(\theta = \theta_{\max})_{pl-\sigma} &= 2pz_0 \left[1.33 + 0.7\left(\frac{\sigma_n}{S_Y}\right) + 1.7 \cdot \left(\frac{\sigma_n}{S_Y}\right)^2\right] \\ pz_{eql}(\theta = \theta_{\max},\ \nu = 0.3)_{pl-\varepsilon} &= 2pz_0 \left[0.8 + 1.5\left(\frac{\sigma_n}{S_Y}\right) + 0.62\left(\frac{\sigma_n}{S_Y}\right)^2\right] \end{aligned} \tag{22}$$

$$\begin{aligned} \theta_{\max pl-\sigma} &= \pm\cos^{-1}\left[0.33 - 0.07\left(\frac{\sigma_n}{S_Y}\right) - 0.25\left(\frac{\sigma_n}{S_Y}\right)^2 + 0.76\left(\frac{\sigma_n}{S_Y}\right)^3\right] \\ \theta_{\max pl-\varepsilon}(\nu = 0.3) &= \pm\cos^{-1}\left[0.053 + 0.84\left(\frac{\sigma_n}{S_Y}\right) - 1.57\left(\frac{\sigma_n}{S_Y}\right)^2 + 1.36\left(\frac{\sigma_n}{S_Y}\right)^3\right] \end{aligned} \tag{23}$$

Note that the above expressions for the maximum angles agree with the expected values for low nominal stresses, i.e., if σ_n/S_Y tends to zero then

$$\begin{aligned} \theta_{\max pl-\sigma} &= \pm\cos^{-1}0.33 \cong \pm 70.5^o \\ \theta_{\max pl-\varepsilon}(\nu = 0.3) &= \pm\cos^{-1}0.053 = \pm\cos^{-1}[(1-2\nu)^2/3] \cong \pm 86.9^o \end{aligned} \tag{24}$$

Note also from Figure 9 that the angle θ_{max} under plane strain decreases in absolute value (because its cosine increases) when the ratio σ_n/S_Y gets higher, a clear indication of the "butterfly effect" on the plastic zone shape. This also happens under plane stress, however only for $\sigma_n/S_Y > 0.3$. Finally, expressions are proposed to fit the shape of the calculated plastic zones:

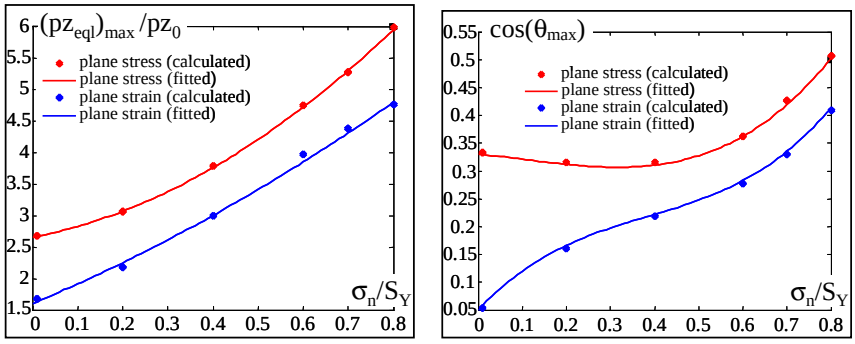

Figure 9: Calculated and fitted values of the maximum normalized plastic zone size $(pz_{eql})_{max}/pz_0$ (left) and associated angle θ_{max} (right), as a function of σ_n/S_Y, for plane stress and plane strain ($\nu = 0.3$).

$$
\begin{aligned}
pz_{eql}(\theta) &= pz_{eql}(\theta_{\max}) - [pz_{eql}(\theta_{\max}) - pz_{eql}(0)]\left[\frac{\cos\theta - \cos\theta_{\max}}{1 - \cos\theta_{\max}}\right]^2, \quad |\theta| \leqslant \theta_{\max} \\
pz_{eql}(\theta) &= pz_{eql}(\theta_{\max}) \cdot \left[\frac{\cos\theta + 1}{\cos\theta_{\max} + 1}\right]^{1+0.8\frac{\sigma_n}{S_Y}} \cdot \left[\frac{\cos\theta - \gamma}{\cos\theta_{\max} - \gamma}\right]^{1-0.8\frac{\sigma_n}{S_Y}}, \quad \theta_{\max} < |\theta| \leqslant \pi
\end{aligned}
\tag{25}
$$

where the auxiliary variable γ is defined as

$$
\gamma \equiv \frac{1 - 0.8 \cdot \sigma_n/S_Y + 2 \cdot \cos\theta_{\max}}{1 + 0.8 \cdot \sigma_n/S_Y} \tag{26}
$$

Finally note that the above expressions are valid for either plane stress or plane strain, as long as the appropriate values of $pz_{eql}(0)$, $pz_{eql}(\theta_{max})$ and θ_{max} presented above are used. The quality of the fitting can be seen in Figure 10 for plane stress and plane strain.

However, these $pz_{eql}(\theta)$ are specific for the Irwin plate, but the same procedure can be applied to estimate the plastic zones of any other geometry for which an appropriate Westergaard stress function is available. Moreover, these estimates can be used for calibrating finite-element plastic zone calculations, which can be quite tricky.

7 Conclusions

The nominal stress to the yield strength ratio, σ_n/S_Y, significantly affects the size and the shape of the plastic zones ahead of crack tips, as demonstrated by the rigorous solution of the Irwin crack problem. Therefore, contrary to what is usually accepted and taught in the traditional LEFM literature, the plastic zones do ***not*** depend only on the magnitude of the stress intensity factor K_I. This

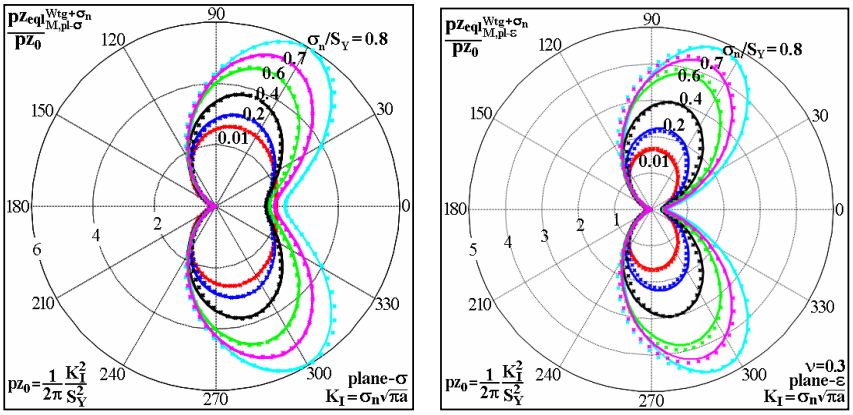

Figure 10: Fitted curves to the Mises plastic zones under plane stress (left) and plane strain (right) considering both the σ_n/S_Y and the equilibrium effects.

fact has important consequences, as it can be used to seriously question the similitude principle, one milestone in the practice of mechanical design against fracture. Thus, it should be better explored and understood.

Acknowledgements

The authors have been partially supported by research scholarships provided by the Brazilian National Research Council, CNPq.

References

[1] Unger, D.J., *Analytical Fracture Mechanics*. Dover, 2001.

[2] Inglis, C.E., Stress in a plate due to the presence of cracks and sharp corners. *Philosophical Transactions of the Royal Society series A*, **215**, pp. 119–233, 1913.

[3] Tay, T.E., Yap, C.N. & Tay, C.G., Crack tip and notch tip plastic zone size measurement by the laser speckle technique. *Eng Fract Mech*, **52(5)**, pp. 879–893, 1995.

[4] Sanford, R.J., *Principles of Fracture Mechanics*. Pearson Education, 2003.

[5] Tada, H., Paris, P.C. & Irwin, G.R., *The Stress Analysis of Cracks Handbook*. ASM, 3rd edition, 2000.

[6] Anderson, T.L., *Fracture Mechanics*. CRC, 3rd edition, 2005.

[7] Newman, J.C., Crews, J.H., Bigelow, C.A. & Dawicke, D.S., Variations of a global constraint factor in cracked bodies under tension and bending loads. *ASTM STP 1244*, pp. 21–42, 1995.